Pulsed Optically Pumped Rb clock with optical detection: first results

Salvatore Micalizio, Aldo Godone, Filippo Levi, and Claudio Calosso

Istituto Nazionale di Ricerca Metrologica, INRIM, Strada delle Cacce 91, 10135, Torino, Italy

Florian Gruet, Matthieu Pellaton, Thejesh Bandi, Christoph Affolderbach, and Gaetano Mileti

Laboratoire Temps – Fréquence (LTF), Université de Neuchâtel, Av. De Bellevaux 51, 2009 Neuchâtel, Switzerland

INTRODUCTION

In this work we present the first results related to a prototype of Rb clock working in pulsed regime, developed in the frame of an ESA contract ("Next generation compact atomic clocks", 21504/08/NL/GLC). The contract is a joint participation between Istituto Nazionale di Ricerca Metrologica, Optics Division (INRIM, Italy) and Université de Neuchatel, Laboratoire Temps – Frequence (LTF, Switzerland).

The contract aims to develop a high performance optically pumped Rb clock using a vapor cell-cavity arrangement. The clock works in pulsed regime: the laser light for the optical pumping, the microwave signal for the interrogation and the detection phase take place at different times. This technique has been demonstrated very effective to reduce light shift and to significantly improve the frequency stability of vapor cell frequency standards.

The apparatus has been designed to detect the clock transition in the optical domain that in principle allows to reach a frequency stability (in terms of Allan deviation) well below 1×10^{-12} at 1s [1]. To achieve this goal, a compact physics structure and a proper electronics have been assembled and tested at INRIM. The physics package is placed under vacuum in order to eliminate the effects of the ambient parameters and to simulate a space environment. An active control of the temperature has been also implemented. The electronics provides a low phase noise microwave signal limiting the clock stability at the level of 1×10^{-13} at 1s and drives all the clock operation through a digital board.

A compact frequency-stabilised laser head generating a radiation at 795 nm for the optical pumping phase has been realized and characterized at LTF. In particular, a relative intensity noise (RIN) as low as 5×10^{-14} Hz^{-1} at 300 Hz has been measured for a laser output power of 45 mW.

The paper is organized as follows: in Section 1 we will describe the physics package and some characterization measurements we have performed on it, Section 2 reports the test we have done on the electronic boards and finally Section 3 is devoted to the characterization of the laser system.

PHYSICS PACKAGE

The advantage of the pulsed technique applied to vapor cell frequency standards and the results obtained with maser approach have been reported elsewhere [1, 2]. We focus this paper on the description and characterization of the three subsystems we implemented. Fig. 1 shows a schematic of the physics package of the Pulsed Optically Pumped (POP) Rb clock.

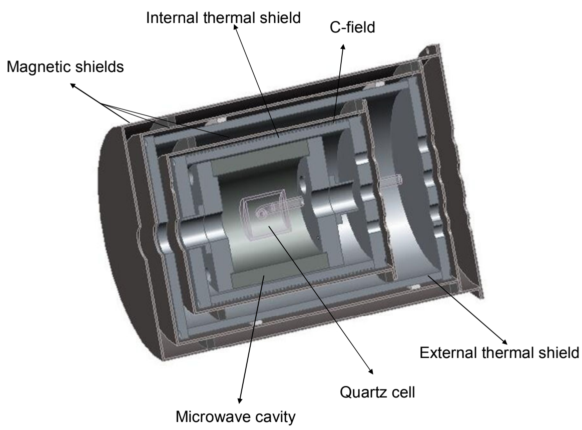

Fig. 1. Physics package of the POP Rb clock

The physics package for the POP with optical detection is designed taking advantage of the experience of the pulsed rubidium maser [2]. It is composed of the following elements: 1) Quartz cell; 2) Microwave cavity; 4) C-field solenoid and magnetic shields; 5) Thermal heaters. In the following we will present a description of the various parts.

Quartz Cell

The cell is made out of quartz in order not to destroy the cavity quality factor. In fact, even in the case of optical detection it is important to maintain a well defined cavity mode in order to achieve the maximum homogeneity in the field parameters. Any inhomogeneity will result in an increased clock sensitivity to external fluctuation, as laser and microwave power noise conversion, temperature sensitivity etc.
The cell has been filled with ^{87}Rb atoms and a temperature compensated mixture of buffer gases (Ar and N_2) in LTF facilities.

Microwave Cavity

The microwave cavity is made of Mo and resonates on the TE_{011} mode at the ^{87}Rb hyperfine frequency (6.834 GHz). The choice of molybdenum is motivated by the following reasons: first, it has a good-enough surface electrical conductivity $\rho = 5\times10^{-8}\ \Omega$ m, and has a thermal expansion coefficient of 5.1×10^{-6}/°C, 4.5 times smaller than Al. The long term relaxation rate of the physical dimension is significantly lower and is estimated to be 10 times smaller than Al. Therefore, the use of Mo for the cavity is expected to increase also the medium-long term performances of the clock.
After few thermal cycles, the loaded quality factor Q_L with the cell inside the cavity is of the order of 1500, probably due to a thin film deposition of Rb atoms on the inner surfaces of the cell. However, contrary to the maser approach, the detection of the clock signal in the optical domain does not require a very high Q_L; indeed, a low Q_L results in a low cavity pulling.
An active control of the cavity tuning has been implemented by coupling to the cavity a varactor diode working in reversed bias condition. The cavity can be then finely tuned and the range of tuning is of the order of 500 kHz (Fig. 2).

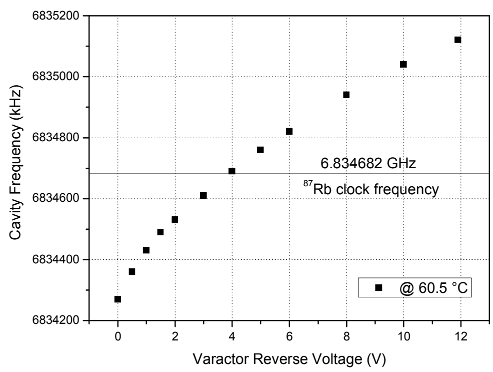

Fig. 2. Cavity tuning through a varactor diode.

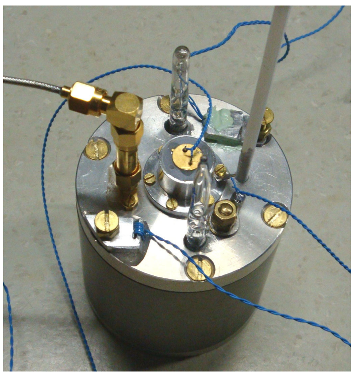

Fig. 3. The cavity system.

The cavity system includes also the detection optics that is designed to focalize the detection laser beam into a photodiode.
Fig. 3 shows the cavity system we implemented. Among others, it is possible to distinguish the two cell tails coming out of the cavity, the photodiode, the varactor housing, and the tuning screw.

C-Field, Heaters and Magnetic Shields

The first enclosure outside the cavity is a cylinder made of aluminum and serves two purposes: 1) C-field generation to maintain a uniform field in the z-direction (along the direction of the pumping laser) for Zeeman splitting of the transition levels. The C-field solenoid is wrapped with a pitch of 2 mm, generating a field of 6 mG/mA; 2) a heating element (Minco kapton adhesive thermofoil heater) is attached to the outside of the cylinder, which maintains the operating temperature of 65 °C inside the cavity.

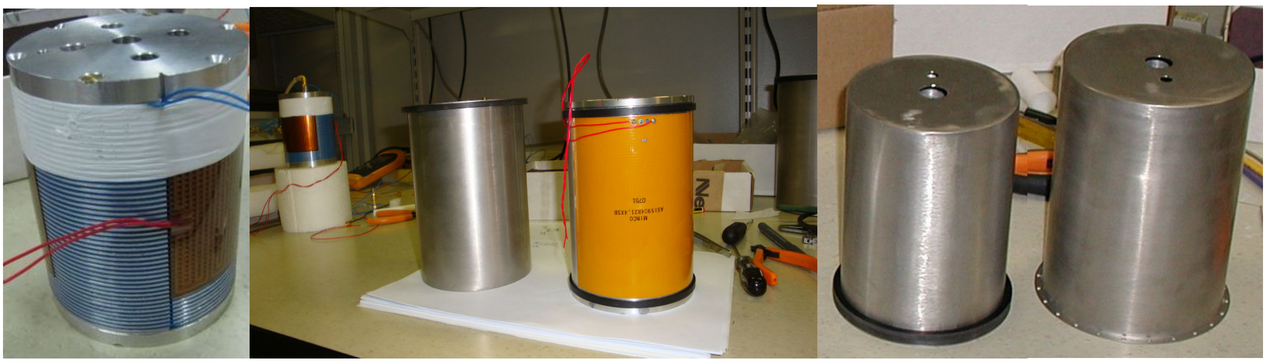

Fig. 4. Form left to right: C-field coils (in blue) and inner heater; first magnetic shield and external heater; the outmost magnetic shields.

The heater is driven with AC RF source (at 40 kHz) to nullify the residual magnetic field generated by the heater. The C-field current is about 1 mA. At this level, a relative current fluctuation of 3×10^{-5} causes a frequency instability of 10^{-15}.
After the first heater around the cavity, there is a first magnetic shield that in turn is placed inside the second heater. Two magnetic shields complete the physics package. By using three magnetic shields, a reduction of 10^3 of the longitudinal field is estimated. This gives a frequency shift of $< 3\times10^{-13}$/G for a quantization magnetic field of 10 mG.
The tails of the cell are connected by copper loops to the second heater to ensure that the temperature of the tails are maintained below that of the cell volume. A minimum of 5 °C gradient should be maintained between the cell volume and the cold finger to avoid the accumulation of the metallic rubidium in the cell. The second and third μ-metal shielding are shown in the Fig. 4.
The physics package is housed in a vacuum enclosure with the aim to warrantee the highest isolation from environmental fluctuations as well as to test the physics package in a space-like environment. In particular we are interested in the behavior of the temperature stabilization systems, of the insulation requirements in absence of air convection and finally in the behavior of the microwave cavity. The environment pressure fluctuation is in fact responsible of a change in the refraction index of the air; in particular, a variation of 1 Pa produces a variation of the refraction index of -2.3×10^{-9}; this variation causes a cavity resonance change of about -15 kHz/ Pa.

Characterization measurements

Several characterization measurements have been done on the physics package. Here we report the observation of the Ramsey fringes and measurement of the frequency stability. Both these measurements have been done using the apparatus in the maser configuration, being the electronics for the detection in the optical domain not yet assembled to the physics package.
Fig. 5 shows the Ramsey fringes obtained for a cavity temperature of 64 °C; at this temperature and for the our cell sizes the longitudinal and transversal relaxation rates are γ_1 = 230 s^{-1} and γ_2 = 240 s^{-1} respectively. They have been measure with the free induction decay technique [3].
For optical pumping purposes, we used a DFB laser tuned to 795 nm (D_1 line of ^{87}Rb) with a power of 2.2 mW at the cell entrance. The timing used for Fig. 5 is t_1 = 400 ms, T = 4.2 ms, t_p = 4 ms, t_d = 2 ms, being t_1 the duration of each

microwave pulse (Rabi time), T the Ramsey time, t_p and t_d the duration of the laser pumping phase and of the detection phase respectively.

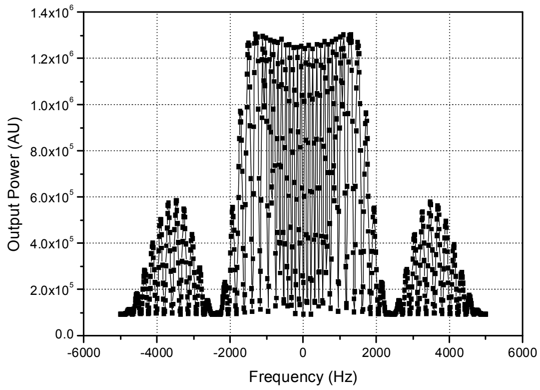

Fig. 5. Ramsey fringes observed in the microwave domain (POP maser). The linewidth of the central fringe is 50 Hz.

Fig. 6 is a measurement of the POP maser frequency stability in terms of Allan deviation. The short term frequency stability of 7×10^{-12} at 1 s is due to the low cavity quality factor, as previously mentioned. Moreover, the figure shows that the white frequency region extends up to 100000 s, reaching the value of 2×10^{-14}, without removing a linear drift from the data.

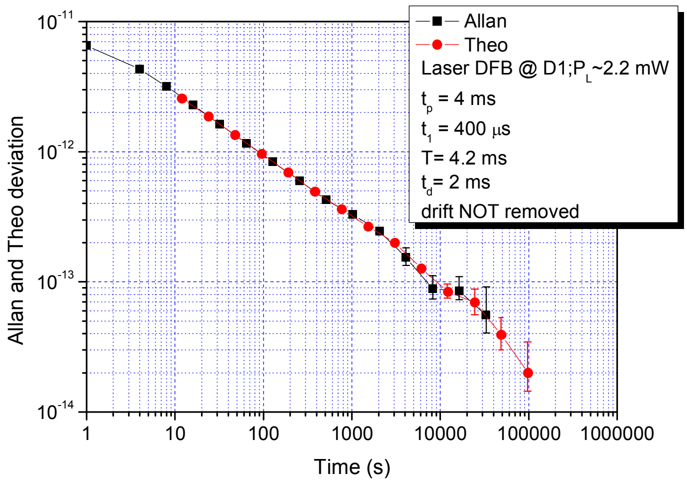

Fig. 6. Allan and Theo deviation of the POP maser clock.

ELECTRONICS

A dedicated electronics has been designed in order to provide a low-phase noise microwave signal at 6.834 GHz starting from a local oscillator (LO) at 10 MHz and to lock the LO to the atomic signal [4]. A scheme of the clock electronics is reported in Fig. 7. Another goal of the electronics is to control some parameters whose fluctuations can affect the resonance frequency, such as the environmental temperature.

The implemented boards have been tested. We report here the characterization of the synthesis chain branch going from 10 to 180 MHz. The first multiplier (x9) gives the main contribution to the synthesis chain noise. It is followed by a doubler (x2). To reduce the effect of the spurious a VCO is phase locked to the line of interest. The bump is due to filtering the VCO at 180 MHz.

Fig. 8 shows that for the frequency of interest (around 100 Hz) the noise of the synthesis chain is below the value required in order to have an overall contribution to the clock stability at the level of $1\text{-}2\times10^{-13}$ at 1s.

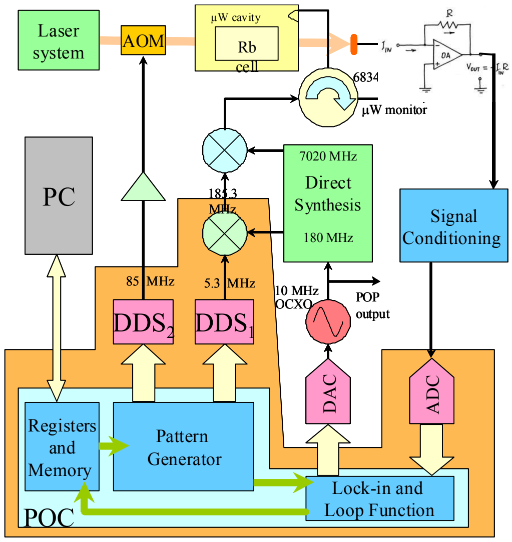

Fig. 7. The POP clock with optical detection from an electronic point of view.

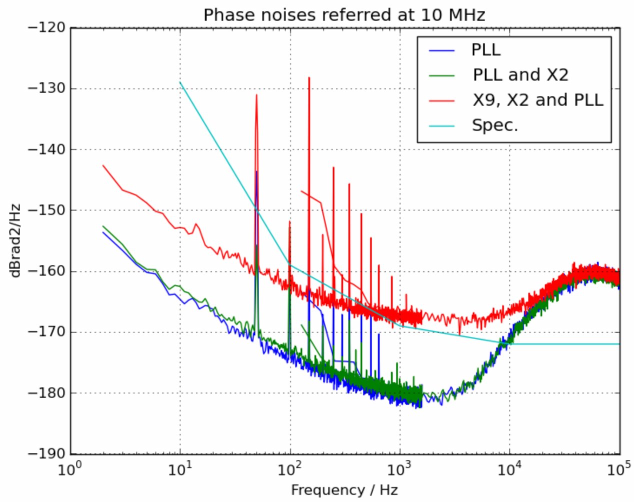

Fig. 8. Phase noise of the synthesis chain.

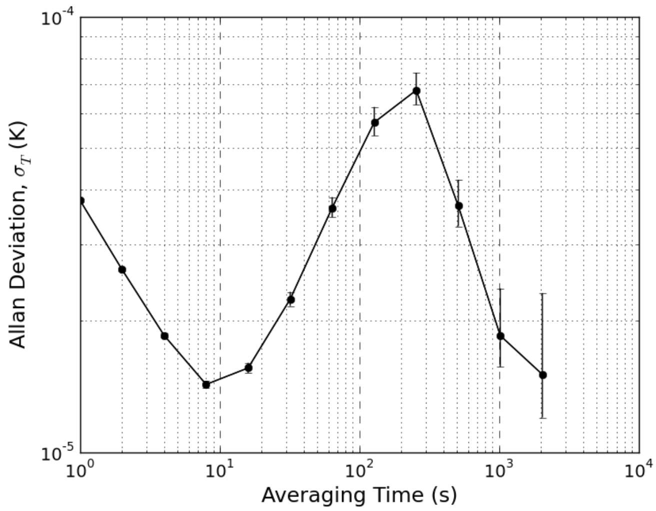

Fig. 9. Allan deviation of the temperature of the external heater (54 °C).

The photodiode and the trans-impedance amplifier used for the optical detection have been characterized; the trans-impedance, in particular, has been designed to detect laser power in the range 1-10 mW. The noise level introduced by the trans-impedance is 10 dB below the shot noise limit corresponding a 1 mW.
The pulsed operation, that is about 100 times faster than that of an atomic fountain, is guaranteed by a FPGA that coordinates and runs all the clock operation phases.
Since there are several temperature-dependent physical phenomena affecting the clock frequency (buffer gas, spin exchange, cavity pulling) an active double temperature control has been implemented.
Fig. 9 shows the temperature stability of the external heater as measured by a monitor Negative Temperature Coefficient (NTC) sensor. It turns out that the external temperature is stable at the level of 100 μK. The stability of the cavity (internal heater) is expected to be at least a factor of ten better.

STABILIZED LASER HEAD

Laser Properties

Our Laser Head uses a DFB laser diode at 795 nm from Eagleyard Photonics. It is mounted in a TO3 can with an integrated Peltier, which allows an excellent temperature stabilisation. Properties of the laser after characterization are given in Table 1. Fig. 10 shows the detailed measurement of Relative Intensity Noise (RIN) and Frequency noise (FM noise).

Table 1. Characterized laser properties.

Parameter	795 nm DFB
ν(I) [GHz/mA]	1
ν(T) [GHz/K]	25
Rb reached	Yes
Single mode operation	Yes
Output power [mW]	> 60 (laser output)
SMSR [dB]	> 45
RIN [Hz^{-1}]	$5*10^{-14}$ @ 300 Hz (45 mW output power)
FM noise [kHz/√Hz]	4 @ 300 Hz
Linewidth [MHz]	< 4 MHz

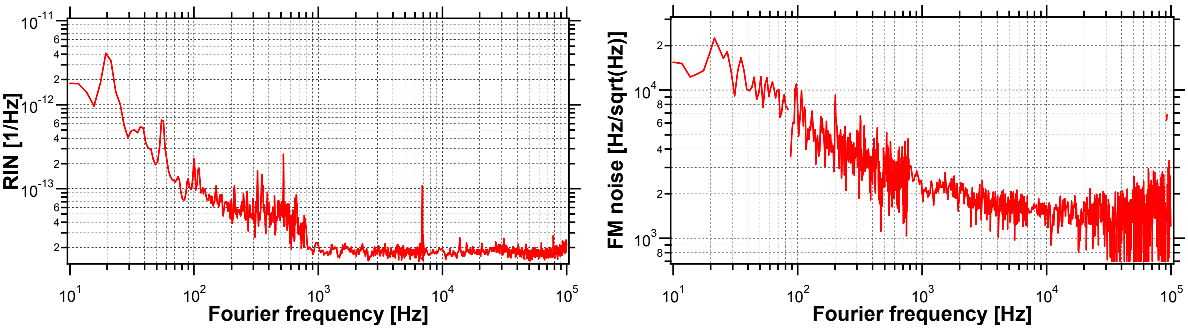

Fig. 10. RIN and FM noise of the characterized DFB laser.

Laser Head Assembly

Fig.11 shows the fully assembled Laser Head, based on [5]. The laser's frequency is stabilized using sub-doppler absorption peak of a thermally stabilized home-made reference rubidium cell. Overall volume of the Laser Head is 0.65 litres (100 mm x 100 mm x 65 mm), of which approximately 1/3 is occupied by the laser and optics hardware.

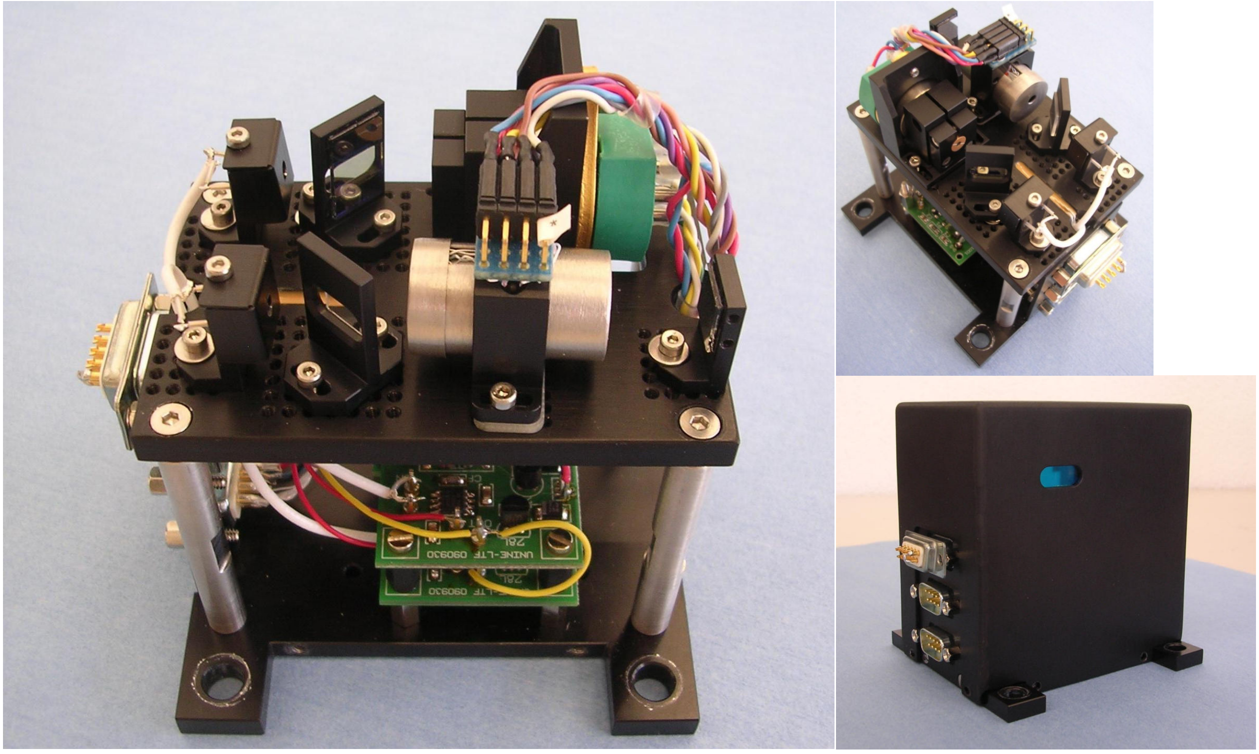

Fig. 11. Pictures of the fully assembled Laser Head.

Laser Head Frequency Stability

The Laser Head frequency stability has been measured by beat note between two 795 nm stabilized Laser Heads. Each Laser Head is locked on two different ^{87}Rb transitions distant of about 817 MHz (Fig. 12.b) and the beat frequency is then measured through a fast photo-detector and a frequency counter. Concerning the stability measurement showed in Fig. 12.a, the reference cells were not yet heated nor thermally stabilized, which results on some frequency drift. Still, the frequency stability is better than 10^{-10} at all timescales from 1 second up to 1 day.

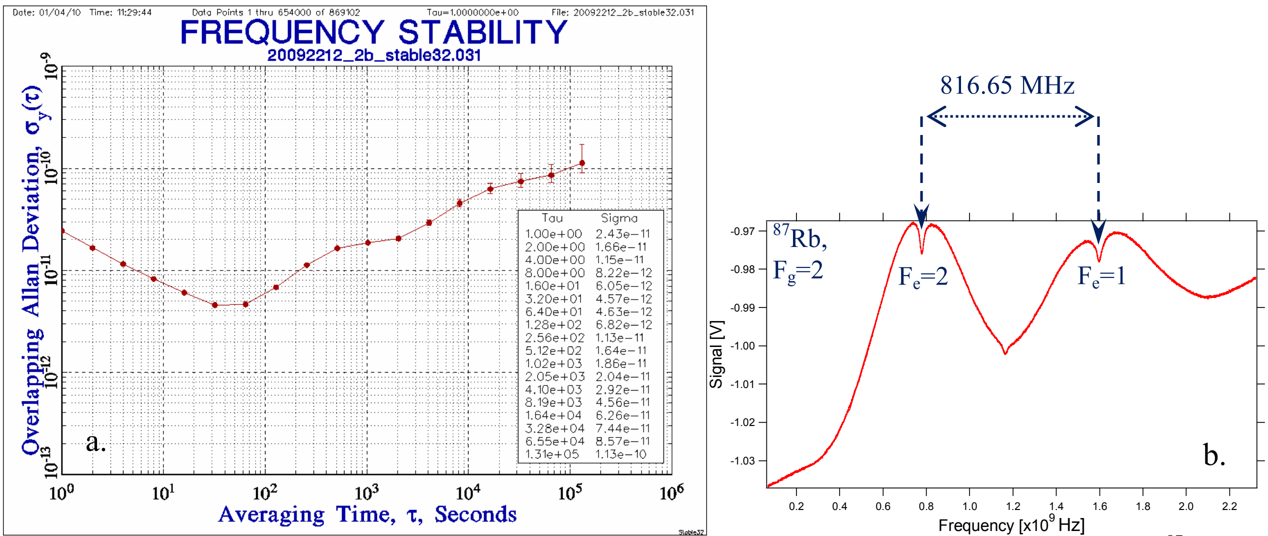

Fig. 12. a. Allan deviation of the frequency stability measurement; b. Saturated absorption spectrum of ^{87}Rb.

Rubidium Cell Production at LTF

Heart of the physics package and of the laser head, rubidium cells have been produced in our laboratory. Our cell filling system allows us an excellent control of the atmosphere inside the cells. The PP cell is made of quartz and contains ^{87}Rb plus a buffer gas mixture, chosen precisely according to the PP requirements.
The reference cell for the laser head also contains enriched ^{87}Rb, but is otherwise evacuated. Care is taken to avoid contamination with residual gases inside the cell, that would directly deteriorate the quality of the saturated absorption spectrum. Our process allows us a good control on this residual gas contamination, and thus, the production of excellent stabilisation cells.

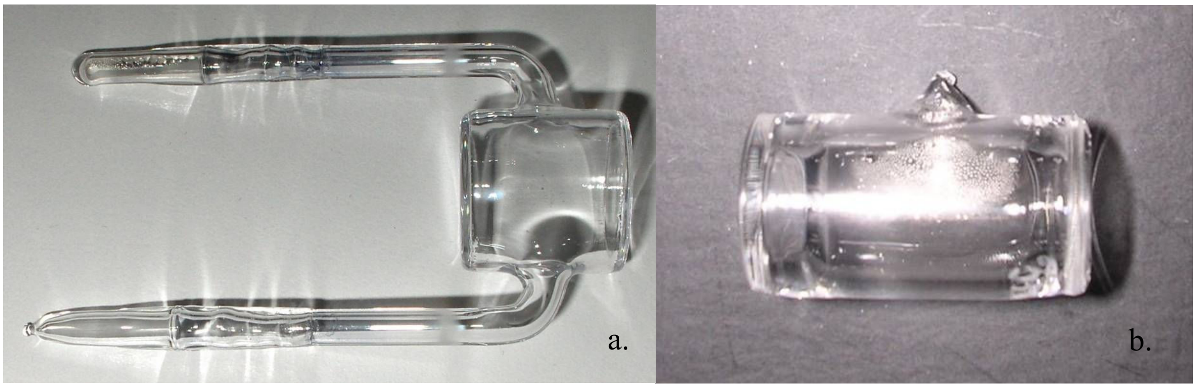

Fig. 13. a. PP cell. Dimensions: Ø20 mm x 20 mm length. b. Laser head stabilization cell. Dimensions: Ø 10 mm x 19 mm length.

The PP and the Laser Head are now mounted and ready to be assembled. Next step will be to assemble them together and start clock stability measurements.

ACKNOWLEDGMENTS

We acknowledge financial support by the European Space Agency (ESTEC contract 21504/08/NL/GLC), the Swiss Space Office and the Swiss National Science Foundation (grant 200020-105624, CRSI20-122693/1). We thank our colleagues R. Matthey, P. Scherler and M. Durrenberger (all at LTF-UniNe) for their contributions.

REFERENCES

[1] S. Micalizio, A. Godone, F. Levi, and C. Calosso, “Pulsed optically pumped ^{87}Rb vapor cell frequency standard: a multilevel approach”, *Phys. Rev. A*, vol. 79, pp. 013403 (1-19), January 2009.

[2] A. Godone, S. Micalizio, F. Levi, and C. Calosso, “Physics characterization and frequency stability of the pulsed rubidium maser”, *Phys. Rev. A*, vol. 74, pp. 043401 (1-12), October 2006.

[3] J. Vanier and C. Audoin, *The Quantum Physics of Atomic Frequency Standards*, Adam-Hilger, Bristol, p. 1043, 1989.

[4] C. Calosso, S. Micalizio, A. Godone, and F. Levi, “Electronics for the pulsed rubidium clock: Design and characterization”, *IEEE Trans. Ultrason. Ferroelect. Freq. Control*, vol. 54, pp.1731-1740, September 2007.

[5] C. Affolderbach, G. Mileti, "A compact laser head with high frequency stability for Rb atomic clocks and optical instrumentation", *Review of Scientific Instruments 76*, 073108, 2005.